

1 *Article*

2 **Microdrop Deposition Technique: Preparation and** 3 **Characterization of Diluted Suspended Particulate** 4 **Samples**

5 **S. Macis^{1,2*}, G. Cibin³, V. Maggi^{4,5}, G. Baccolo^{4,5}, D. Hampai², B. Delmonte⁴, A. D'Elia⁶ and A.**
6 **Marcelli^{2,7}**7 ¹Department of Mathematics and Physics, Università di Roma Tor Vergata, via della Ricerca Scientifica 1,
8 00133, Rome, Italy9 ²Istituto Nazionale di Fisica Nucleare - Laboratori Nazionali di Frascati, 00044, Frascati, Italy10 ³Diamond Light Source, Harwell Science and Innovation Campus, OX11 0DE, Didcot, Oxfordshire, UK11 ⁴Dipartimento di Scienze dell'Ambiente e della Terra, Università degli Studi di Milano Bicocca, Piazza della
12 Scienza, 1 – 20126, Milano13 ⁵Istituto Nazionale di Fisica Nucleare, Sezione di Milano-Bicocca, Piazza della Scienza, 3 – 20126, Milano14 ⁶Department of Physics, University of Trieste, Via A. Valerio 2, 34127 Trieste, Italy15 ⁷Istituto Officina dei Materiali, Consiglio Nazionale delle Ricerche, Basovizza SS-14, km 163.5, 34149 Trieste,
16 Italy

17 *Correspondence: salvatore.macis91@gmail.com; Tel.: +39 0672594523

18 **Abstract:** The analysis of particulate matter (PM) in dilute solutions is an important target for
19 environmental, geochemical and biochemical researches. Here we show how the microdrop
20 technology may allow to control, through the evaporation of small droplets, the deposition of
21 insoluble materials dispersed in a solution on a well-defined area with a specific spatial pattern.
22 Using this technology the superficial density of the deposited solute can be accurately controlled. In
23 particular, it becomes possible to deposit an extremely reduced amount of insoluble material -in the
24 order of few μg - on a confined area, thus allowing a relatively high superficial density to be reached
25 within a limited time. In this work we quantitatively compare the microdrop technique for the
26 preparation of particulate matter samples with the classical filtering technique. After having been
27 optimized, the microdrop technique allows to obtain a more homogeneous deposition and limit
28 sample consumption of a factor ~ 25 . This method is potentially suitable for many novel applications
29 in different scientific fields.

30 **Keywords:** ultra-dilution; droplets; water; evaporation; X-ray fluorescence

31

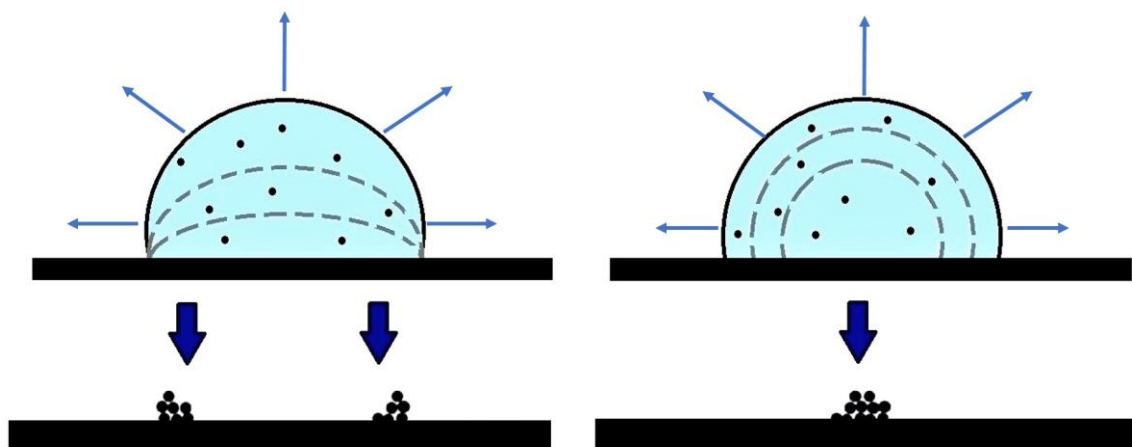
32 **1. Introduction**

33 When dealing with complex samples, one of the main bottlenecks from the practical point of
34 view is their preparation. A suitable sample preparation method should allow saving time during
35 data acquisition, enhancing the S/N ratio, improving the detection limits, etc. Considering particulate
36 matter (PM) analysis of solutions, the most common preparation technique is filtration: it is easy,
37 reliable and fast, but at the same time it presents some drawbacks. Indeed, it requires a considerable
38 sample consumption and PM whose size is smaller than the one of the filtration pores, are not
39 retained on the filter. To avoid this point, the original solution could be deposited on a membrane
40 presenting a quite large surface (about 1 cm^2). In this case a critical issue is the low superficial density
41 of the PM deposited on top of it.

42 The evaporation process, based on the deposition of micro-droplets, may overcome both issues.
43 Indeed, the microdrop technique consists in the deposition of PM in association to liquid drops
44 presenting a diameter between 70 and 200 μm . After the evaporation of the solvent, the PM
45 depositional pattern resembles the one of the original droplets. The main disadvantages of this
46 method are the inhomogeneity of the deposition and the long time required for the evaporation of
47 the solvent. In fact, the evaporation of large drops (few mm of diameter) can last several hours. At

48 normal conditions of temperature and humidity, full evaporation of drops of water can require more
 49 than 10 hours per ml and the density fluctuation of the deposited material is up to 80% as a
 50 consequence of the so called coffee-stain effect [2]. To optimize the process, we deposit micro-droplets
 51 and control the deposition area with motorized translational stages. To this purpose a study of the
 52 evaporation dynamics is necessary to investigate the uniformity of deposition and to evaluate the
 53 evaporation rate of micro-droplets presenting different sizes. When dealing with densely packed
 54 deposition patterns our results show that is necessary to consider the interaction between different
 55 evaporating droplets.

56 The evaporation of a drop on a surface can be described with two different models: the
 57 evaporation with a “constant contact area” and that with a “constant contact angle” [1] (see figure 1).



58
 59 Figure 1: Deposition and evaporation processes for two different models: “constant contact area” (left) and
 60 “constant contact angle” (right). The main difference is represented by the shape of materials deposited on the
 61 substrate: pinned at the edge for the “constant contact area” model (bottom left) and concentrated in the center
 62 for the “constant contact area” model.
 63

64 In the first case, the evaporation takes place maintaining a constant contact area between the
 65 liquid drop and the surface. The shape of the drop remains almost “spherical” [1], but the contact
 66 angle decreases. In accordance to the second model, the contact angle of the edge of the drop is
 67 constant during the evaporation [2], thus the shape of the drop remains “spherical” but the contact
 68 area between liquid and surface continuously decreases. The “constant contact area model” is
 69 suitable when a strong interaction between the liquid and the substrate takes place, as when
 70 considering water and a hydrophilic surface [3,4]. On the opposite, the second model is more
 71 appropriate when the drop-substrate interactions are weak, as in the case of water on a hydrophobic
 72 substrate.

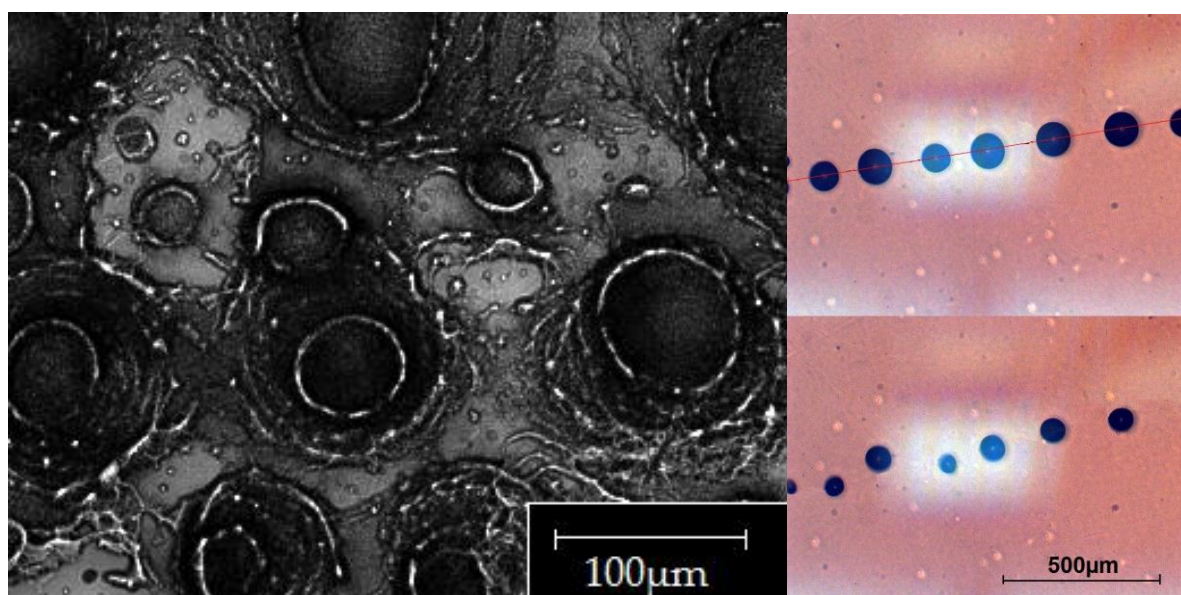
73 In this contribution we will describe the optimization process of an experimental setup based on
 74 the evaporation of water micro-droplets in accordance to the constant angle model. The uniformity
 75 of the deposition will be determined and the results will be compared to the ones obtained through
 76 a classical filtration technique.

77 2. Experimental

78 Using a micro-dispenser, micro-sized droplets can be deposited controlling the spatial distribution
 79 of drops, their size and the deposition rate. The Microdrop technology [5] allows spreading extremely
 80 small amounts of a liquid solution. Moreover, thanks to dedicated devices, it is possible to deposit
 81 single droplets whose volume is in the sub-nanoliter range. Such small droplets present an interaction
 82 with the substrate, which can be considered negligible. A micro-dispenser is composed of a head with
 83 a nozzle and a pumping chamber working with the same piezoelectric technology used for inkjet
 84 printers. The head is controlled by a driver, i.e., a pulse generator, which controls the piezoelectric
 85 actuator and sends pulses to the head. The device we used is the MD-K-130 (© Microdrop
 86 Technologies), with an inner nozzle diameter of 70 μm that produces droplets with a minimum

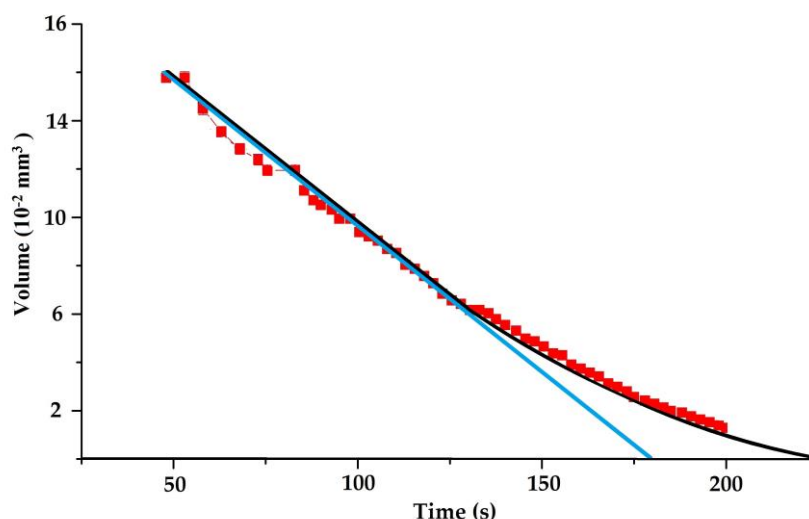
87 volume of 180 pl and a tunable drop rate from 1 to 2000 Hz. To prepare a sample with a specific
88 microdrop pattern, it is necessary to control the number of drops on the substrate, releasing each of
89 them at a well-defined and repeatable distance. In our experimental setup, to generate the pattern,
90 the head is maintained fixed while the substrate translates under the stream of droplets released by
91 the head. The motion of the substrate is realized with two precision PI Micos Translational Stage VT-
92 80 stages, assembled perpendicularly with respect to each other. This setting allows positioning the
93 substrate with a nominal accuracy of 1 μm per axis. The desired spatial patterns are obtained
94 controlling the two translation stages with a LabView© based code and properly setting the
95 Microdrop dispenser [6].

96 The characterization of the evaporation time and of the drop pattern was made with an optical
97 microscope coupled to a video camera. The evaluation of the PM deposition uniformity has been
98 performed using the x-ray fluorescence technique on the B18 beamline at the *Diamond Light Source*
99 facility [7], using a monochromatic x-ray beam at 8 keV and with a focus of 100x100 μm^2 .
100



101
102 Figure 2: Optical microscope image taken at 20x magnification of a microdrop deposition of an ink solution (left).
103 On the right two microscope images taken at 5x magnification of an evaporating line of droplets: one at the
104 beginning of the evaporation (top right) and the second after 10 seconds (bottom right).
105

106 The evaluation of the evaporation was carried out measuring the diameter and height of droplets
107 as a function of time using the optical microscope and the camera. We measured the parameters of
108 the single droplets and of groups of droplets to evaluate the evaporation rate as a function of the size
109 and of the distance between several droplets. We then identified the minimum deposited area
110 achievable with the evaporation of small droplets, in the shortest time. To optimize the deposition
111 process, all images and experimental parameters were analysed and used to write an approximate
112 model.

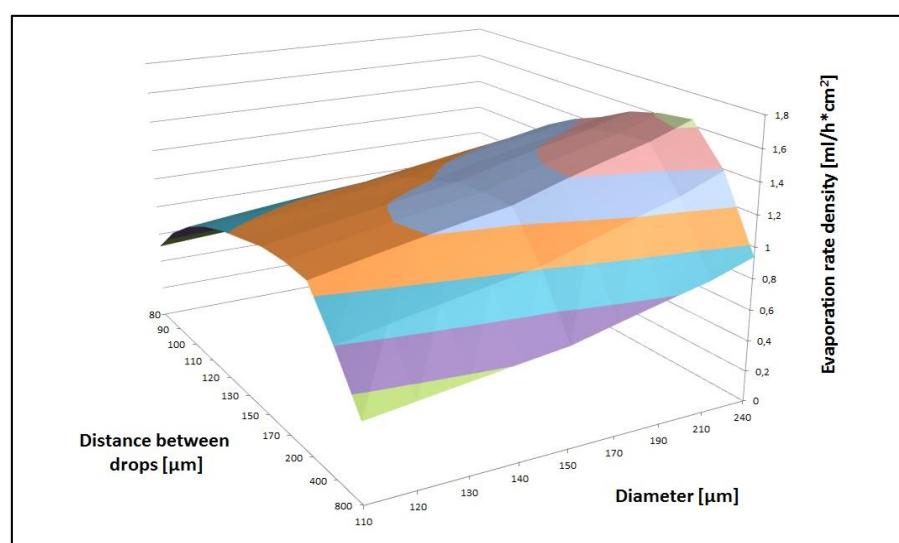


113
 114 Figure 3: Comparison among the droplet mass behavior for the evaporation at “constant contact area” (blue
 115 line), at “constant contact angle” (black line) and experimental data (red squares) of a droplet of a bi-distilled
 116 water solution with an initial diameter of 1 mm, at room temperature.

117 3. Results

118 The analysis of the images of the droplets (see Fig. 2) and of the measured parameters, clearly
 119 points out that using a low concentration solution and a hydrophobic substrate as *Kapton*, the
 120 evaporation occurs in accordance to the “constant angle” model, well described by the theoretical
 121 model introduced by Picknett and Bexon in 1977 [1]. The result is confirmed in Figure 3, where our
 122 data are compared to the “constant angle” and “constant contact area” models. The deposition rate,
 123 i.e., the volume of the liquid deposited vs. time, was optimized considering the velocity of the stages
 124 and the spatial pattern parameters of the deposited droplets. Indeed, a fundamental parameter that
 125 drives the evaporation, is the saturation of the atmosphere surrounding the droplets selves, which is
 126 directly related to the mutual position of the droplets. Different droplet sizes and different distances
 127 between successive droplets were considered to this aim. Detailed results presented in Figure 4 point
 128 out that the highest evaporation rate at 20° C (~ 0.7 ml/h cm²) is obtained setting the droplet diameter
 129 at 240 μm and the distance between two consecutive droplets at 170 μm.

130



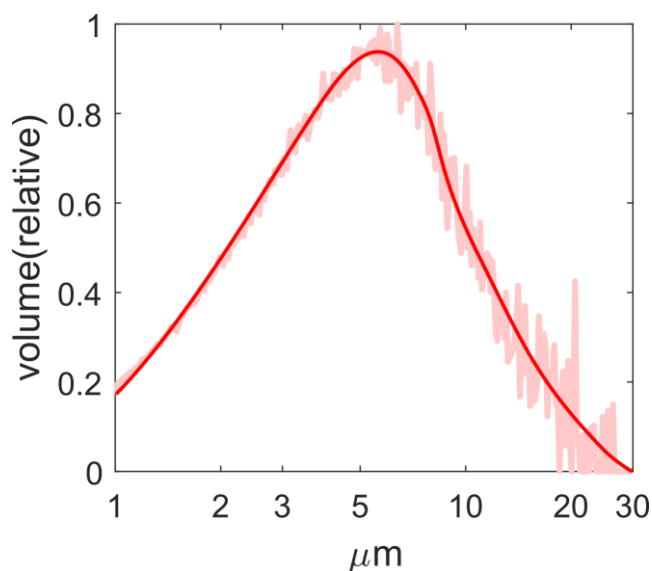
131
 132 Figure 4: Graph of the volume evaporated per hour and of the area vs. the drop diameter and the distance
 133 (among two consecutive drops) at 20° C. To calculate the volume evaporated vs. time and the area we considered
 134 also the speed and the delays of the motorized stages.

135 Closer drops would determine a higher relative humidity in the air layers which surround the drops
136 selves, slowing the evaporation process. On the opposite placing drops at larger distance would limit
137 the amount of deposited liquid with respect to the considered area, reducing the integrated efficiency
138 of the process.

139 To further increase the evaporation rate, experiments conducted heating the substrate were also
140 carried out. As expected, increasing the temperature evaporation rate increase following a power law
141 with exponential value of the temperature of ~ 2.5 . For example at 80°C the evaporation rate increases
142 about 30 times [6]. However, it is worth noting that increasing temperature could not be always
143 feasible, since increasing the temperatures the chemical stability of the samples may be affected. To
144 avoid the problem, thermal radiation focused on droplets may be considered. Selecting specific
145 wavelengths or frequencies it would be possible to selectively increase the temperature of the solvent
146 and not the one of the PM contained in the solution. Another parameter, which could be modified to
147 fasten the deposition, is the speed of the two motorized stages. Our experiments were all conducted
148 at the maximum allowed speed (i.e., $13\text{ mm}\cdot\text{s}^{-1}$), but faster motorized stages exist that allow to cover
149 the same area with a shorter time.

150 To better understand the deposition pattern of the PM contained in a liquid solution deposited
151 with a Microdrop dispenser, we prepared a suspension consisting in high purity water (MilliQ
152 technology) and a given amount ($50\text{ }\mu\text{g}/\text{ml}$) of a reference material: the NIST standard 2709a. The
153 latter is a well-known soil reference material with a well characterized composition [8] and grain size
154 distribution. To avoid the clog of the Microdrop nozzle we selected a reference material whose
155 particles didn't exceed $30\text{ }\mu\text{m}$, i.e., about the half of the aperture of the nozzle orifice, as showed in
156 Figure 5.

157



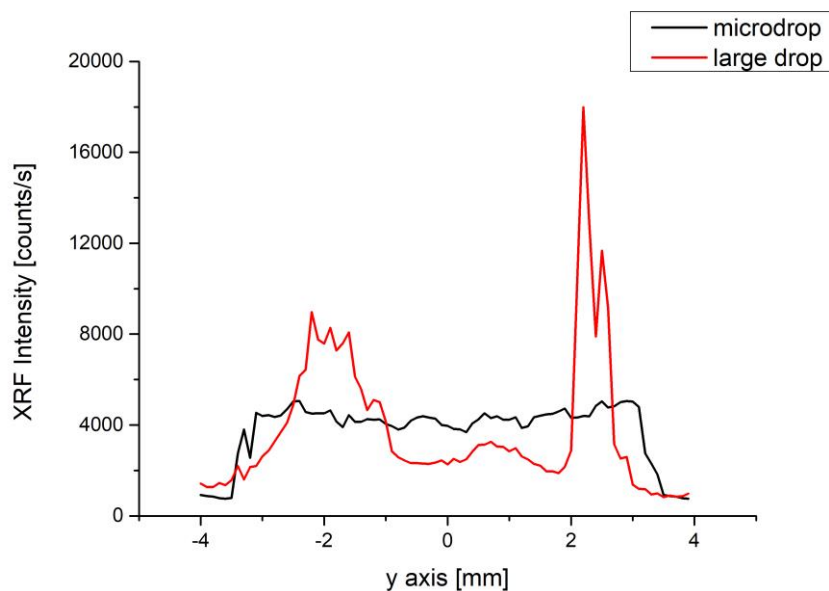
158

159 Figure 5: The particle size distribution of the NIST standard reference soil material 2709a. Data were obtained
160 through the Coulter counter technique. Details can be found in Ref. [10].

161

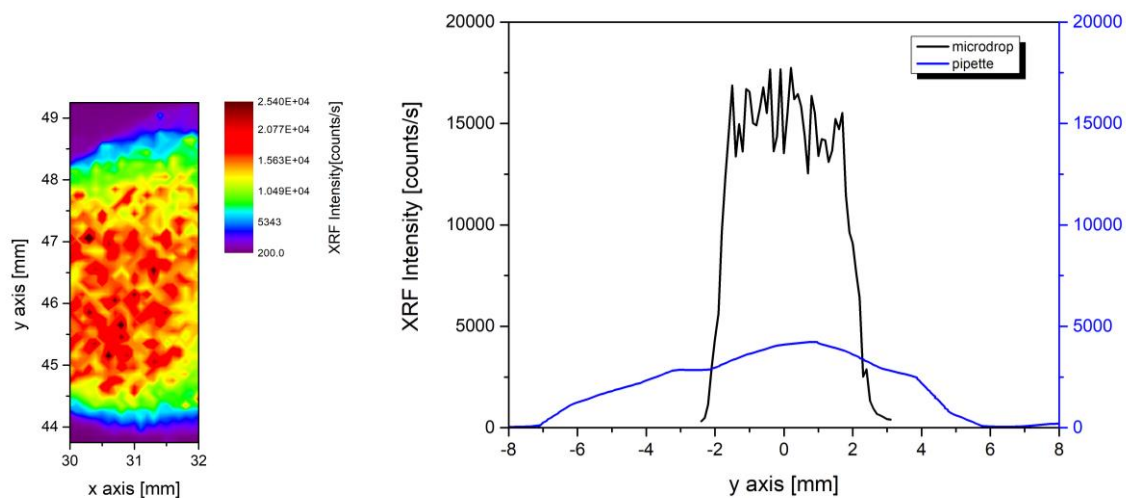
162 Since the standard contains Fe, it was possible to use the X-ray fluorescence (XRF) technique to
163 investigate its spatial distribution after deposition. In Figure 6 we compare two XRF profiles collected
164 on two deposited samples, measured along a straight line. The red curve is the profile relative to the
165 deposition of a single large drop of $\sim 1\text{ ml}$ volume of the NIST solution. The black curve refers to a
166 deposition obtained with the microdrop. The same total volume and the same solution were
167 considered. The two profiles show significant differences and it is remarkable the homogeneous
168 deposition obtained with the latter technique, despite the reduced amount of solution. Indeed, the
169 large drop shows density fluctuations from 50% to 80% of the fluorescence intensity, in particular
170 at the edge due to the coffee-stain effect [2]. At variance the variability observed along the microdrop
171 profile is around 10% and the deposited soil is uniformly distributed.

172 Figure 6 clearly shows that the homogeneity and the overall quality of the samples prepared
 173 with the microdrop increase. The only disadvantage of this method is the deposition time. Indeed, as
 174 it can be inferred from Figure 4, the optimal configuration of this micro-deposition allows to deposit
 175 and to evaporate liquid samples with a rate of less than 1 mL per hour. A simple and alternative way
 176 to reduce the deposition time can be obtained combining the microdrop deposition with a
 177 simultaneous filtering technique. In this way the droplet is deposited onto a wettable filter and the
 178 liquid is pumped out by a vacuum pump.



179 Figure 6: Comparison of two representative X-Ray Fluorescence profiles at the Fe K-edge: microdrop (black) and
 180 a single large drop (red) deposition of a NIST solution using ~1 ml volume.
 181
 182

183 In Figure 7 (left) the 2x5 mm² image shows a portion of the original 4x4 mm² microdrop deposition
 184 area of 1 ml NIST solution (50 µg/ml concentration) on a polycarbonate Nucleopore® membrane filter
 185 (pore size 0.45 µm and filter area diameter ~ 20 mm), which is a hydrophilic substrate. The color map
 186 was obtained collecting the XRF signal at the Fe K-edge. Colors highlight an area of approximately
 187 2x3 mm² where a controlled distribution is achieved. The internal variability is probably also related
 188 to the spatial pattern of the pores characterizing the filtration membrane.
 189



190 Figure 7: Image of the X-Ray Fluorescence at the Fe K-edge of the microdrop deposition area on the filter (left);
 191 comparison of two XRF profiles (right): the microdrop deposition (black) and the pipette deposition (blue) both
 192 achieved with a simultaneous vacuum filtration technique.
 193
 194

195 In Figure 7 (right) one microdrop deposition profile of the image on the left is compared with an
196 analogous profile of the deposition of the same solution using a micro-pipette on the same type of
197 filter. From the analysis of the data, we may point out that using the microdrop deposition ~80% of
198 the material is distributed quite homogeneously (with a fluorescence intensity fluctuation of ~15%)
199 inside an area of ~8 mm². Using the pipette deposition the same amount of material is deposited
200 within an area six times larger (~50 mm²).

201 Conclusions

202 The microdrop technology is suitable to prepare homogeneous deposition of particulate and granular
203 matter samples. In order to establish a reliable procedure, reducing also the deposition time, it is
204 necessary to measure accurately the evaporation rate of the pattern depositions. We show here how
205 to optimize such parameters, increasing the S/N ratio and the deposition homogeneity reducing at
206 the same time the sample consumption. In terms of deposition uniformity, the microdrop technique
207 allows reducing of a factor ~5 the heterogeneity with respect to a classical filtration method. At the
208 same time the S/N ratio may improve ~4 times. These features make this technique effective and
209 competitive with respect to many and diverse applications. Among the many, we cite the
210 characterization of aerosols for pollution monitoring purposes, studies of metallic contaminants in
211 polluted water or the investigation of biological diluted materials at ultra-trace concentrations.
212 Besides homogeneity, another important feature of the method proposed here, is the possibility to
213 concentrate in a very reduced area the material contained in an extremely diluted solution or
214 suspension. This makes it possible to consider impurities whose concentrations span from few ppb
215 to hundreds ppm. As an example, the method is suited for the characterization of the inorganic
216 insoluble particulate matter contained in ice core samples for paleoclimatic reconstructions. Ice core
217 dust samples prepared with a microdrop device could be successfully used for both X-rays
218 absorption and X-ray Fluorescence measurements [9,11] and under particular experimental condition
219 also for XRD experiments [12].

220 **Acknowledgments:** This research is a collaboration among *INFN-Laboratori Nazionali di Frascati, Milano Bicocca*
221 *University* and the *Diamond Light Source* facility. The development of the microdrop instrumentation is a project
222 managed by A. Marcelli with the support of *DARST - Department of the Presidenza del Consiglio dei Ministri*, which
223 is gratefully acknowledged. Part of the preparation was done in the *EuroCold* Laboratory at University of Milano
224 Bicocca, founded by Italian National Science Foundation NextData Project. Part of this research was developed
225 at *Diamond*, the UK national synchrotron radiation facility. One of us (S.M.) acknowledges the *Roma Tre*
226 *University* for financial support during his stage at *Diamond*.

227 References

- 228 1. R. G. Picknett, R. Bexon, The evaporation of sessile or pendant drops in still air, *Journal of Colloid and*
229 *Interface Science* 61, 336–350 (1977).
- 230 2. P. Innocenzi, L. Malfatti, M. Piccinini, D. Grosso, A. Marcelli, Stain Effects Studied by Time-Resolved
231 Infrared Imaging, *Anal. Chem.* 81 (2), 551-556 (2009)
- 232 3. H. Hu, R.G. Larson, Evaporation of a sessile droplet on a substrate, *The Journal of Physical Chemistry*
233 *B* 106, 1334–1344 (2002)
- 234 4. F. Girard, M. Antoni, S. Faure, A. Steinchen, Evaporation and Marangoni Driven Convection in Small
235 Heated Water Droplets, *Langmuir* 22, 11085-11091 (2006)
- 236 5. W. Meyer, *Mikroverklebungen aus dem Tintenstrahldrucker*, PLUS, Eugen G. Leuze Verlag, 3/2013,
237 p. 593-598
- 238 6. S. Macis, Preparation and characterization of ultra-diluted samples via micro-deposition of droplets,
239 Thesis Roma Tre University AA 2014-15
- 240 7. J. Dent, G. Cibin, S. Ramos, S.A. Parry, D. Gianolio, A.D. Smith, S.M. Scott, L. Varandas, S. Patel, M.R.
241 Pearson, L. Hudson, N.A. Krumpa, A.S. Marsch and P.E. Robbins, *J. Phys.: Conf. Ser.* 430 012023 – 2013
- 242 8. E.A. Mackey, S.J. Christopher, R.M. Lindstrom, S.E. Long, A.F. Marlow, K.E. Murphy, R.L. Paul, R.S.
243 Popelka-Filcoff, S.A. Rabb, J.R. Sieber, R.O. Spatz, B.E. Tomlin, L.J. Wood, J. H. Yen, L.L. Yu, R. Zeisler,
244 S.A. Wilson, M.G. Adams, Z.A. Brown, P.L. Lamothe, J.E. Taggart, C. Jones, J. Nebelsick, Certification

- 245 of Three NIST Renewal Soil Standard Reference Materials for Element Content: SRM 2709a San Joaquin
246 Soil, SRM 2710a Montana Soil I, and SRM 2711a Montana Soil II, NIST Special Publication 260-172
247 (2010) 39 pages
- 248 9. A. Marcelli, G. Cibin, D. Hampai, F. Giannone, M. Sala, S. Pignotti, V. Maggi, F. Marino, XANES
249 characterization of deep ice core insoluble dust in the ppb range, *J. Anal. At. Spectrom.* 27, 33-37 (2012)
- 250 10. U. Ruth, C. Barbante, M. Bigler, B. Delmonte, H. Fischer, P. Gabrielli, V. Gaspari, P Kaufmann, F.
251 Lambert, V. Maggi, F. Marino, J.R. Petit, R. Udisti, D. Wagenbach, A. Wegner, E.W. Wolff, Proxies
252 and Measurement Techniques for Mineral Dust in Antarctic Ice Cores, *Environ. Sci. Technol.* 42, 5675-
253 5681 (2008)
- 254 11. A. Marcelli, V. Maggi, *Aerosols in snow and ice. Markers of environmental pollution and climatic*
255 *changes: European and Asian perspectives*, Superstripes Press, Rome, Italy ISBN: 9788866830771
256 (2017)
- 257 12. A. D'Elia, G. Cibin, P.E. Robbins, V. Maggi, A. Marcelli, Design and characterization of a mapping
258 device optimized to collect XRD patterns from highly inhomogeneous and low density powder
259 samples, *Nuclear Instruments and Methods in Physics Research B* 411, 22–28, (2017)